EFDA–JET–CP(07)06-06

A. Gondhalekar, F.S. Zaitsev, T.J. Johnson, V.G. Kiptily, A.A. Korotkov,
S.E. Sharapov, D.S. Testa and JET EFDA contributors

Suprathermal Deuterium Ions Produced by Nuclear Elastic Scattering of DT Fusion α-particles and ICRH Driven He^3 Ions in JET Plasmas

Suprathermal Deuterium Ions Produced by Nuclear Elastic Scattering of DT Fusion α-particles and ICRH Driven He^3 Ions in JET Plasmas

JET-EFDA, Culham Science Centre, OX14 3DB, Abingdon, UK

[1]EURATOM-UKAEA Fusion Association, Culham Science Centre, OX14 3DB, Abingdon, OXON, UK
[2]Moscow State University, Faculty of Computational Mathematics and Cybernetics, Moscow 119899, Russian Federation
[3]Association EURATOM-VR, Alfvén Laboratory, Royal Institute of Technology, 10044 Stockholm, Sweden
[4]CRPP, Association EURATOM - Confederation Suisse, EPFL, Lausanne, Switzerland
** See annex of M.L. Watkins et al, "Overview of JET Results ", (Proc. 21 st IAEA Fusion Energy Conference, Chengdu, China (2006)).*

Preprint of Paper to be submitted for publication in Proceedings of the
10th IAEA Technical Meeting on Energetic Particles in Magnetic Confinement Systems,
Kloster Seeon, Germany.
(8th October 2007 - 10th October 2007)

ABSTRACT.

Measurements and simulations of the suprathermal tail of the energy distribution function of deuterium ions in the Joint European Torus are reported. The suprathermal deuterium ion tail was produced by Nuclear Elastic Scattering (NES) collisions between MeV energy (a) DT fusion α-particles, or (b) ICRH driven He^3 minority ions, in deuterium plasmas. Measurements of the line-of-sight integrated energy distribution function of the suprathermal tail of deuterium ions, DT fusion α-particles and ICRH driven He^3 ions were made using a high energy Neutral Particle Analyzer (NPA). The NES or 'knock-on' tail of the deuterium ion energy distribution function was simulated using the FPP-3D Fokker-Plank code which solves the 3-D trajectory averaged kinetic equations in JET geometry while taking into account the NES of the DT fusion α-particles and He^3 projectile ions on deuterium target ions.

The required input energy distribution function of ICRH driven He^3 minority ions was simulated using the SELFO Monte-Carlo code which yields a self-consistent He^3 ion energy distribution. Simulation of plasmas containing the ICRH driven MeV energy He^3 ions revealed that the measured suprathermal tail ion density exceeded by nearly one order of magnitude that expected due to NES of He^3 ions on deuterium ions. The comparison between measurement and simulation in the He^3 ICRH experiments is contrasted with analogous comparison between measurements and simulation of JET plasmas in which 3.5MeV DT fusion α-particles were the projectile ions, where measurement and simulation roughly agreed. We conjecture that secondary NES processes with products of the fusion reaction $D + He^3 \rightarrow p(14.7MeV) + He^4$ (3.6MeV), which are not included in the FPP-3D code simulations, are responsible for the observed excess knock-on deuterium ion tail in the He^3 minority ICRH experiments. Work is in hand to incorporate these second-generation NES reactions into the FPP-3D code. The importance of the above considerations for a complete understanding of ITER plasma behaviour is underlined.

1. INTRODUCTION

- Evidence is presented for suprathermal tail of deuterium ion energy distribution function produced by **N**uclear **E**lastic **S**cattering(NES) of $D+He^3$ fusion products in JET plasmas.
- The possibility of obtaining information about DT fusion α-particles in tokamak plasmas by measuring the suprathermal tail of the energy distribution of heavy impurity ions such as iron, formed due to NES on the α-particles, was first discussed in ref. [1]. This formalism was elaborated and extended to consideration of minority **I**on **C**yclotron **R**esonance **H**eating (ICRH) driven ions in the plasmas in ref. [2].
- First measurements of the suprathermal tail of the deuterium ion energy distribution, formed due to NES on 3.5MeV DT fusion α-particles in JET plasmas, were reported in ref.[3]; the NES driven tail was inferred from measurement using a high energy **N**eutral **P**article **A**nalyzer (NPA). Subsequently a neutron spectroscopy measurement of effects of NES on total neutron emission from the same plasmas was reported in [4], reinforcing the conclusions of [3].

- Simulation of the suprathermal deuterium ion energy distribution function using the FPP-3D Fokker-Plank code, taking into account NES of DT fusion α-particles on the deuterium fuel ions, was reported in ref. [5].
- Here we report measurement of suprathermal tail of the energy distribution of deuterium ions, formed during He^3 minority ICRH of deuterium plasmas. The deuterium and He^3 ion energy distributions were measured using the high energy NPA.
- The NES driven tail of the deuterium ion energy distribution was simulated using the FPP-3D Fokker-Plank code taking into account NES of He^3 ions on deuterium ions.
- The simulations revealed that the measured suprathermal deuterium tail ion density exceeded by nearly one order of magnitude that expected due to NES on He^3 ions alone.
- The comparison between measurement and simulation in the He^3 ICRH experiments is contrasted with analogous comparison between measurements and simulation of plasmas in which 3.5MeV DT fusion α-particles were the projectile ions, where measurement and FPP-3D simulation roughly agreed.
- We conjecture that NES processes with products of the fusion reaction $D + He^3 \rightarrow p(14.7MeV) + He^4$ (3.6MeV), which are not included in the FPP-3D code simulations, may be responsible for the observed excess suprathermal deuterium ion tail in the He^3 ICRH experiments. A full account of the work presented here is given a recent publication [6].

2. EXPERIMENTAL SETUP FOR He^3 MINORITY ICRH AND MEASUREMENTS ON JET

A series of similar plasma pulses was used for this study. The toroidal field was $\cong$ 3.45T, plasma current $\cong$ 1.8MA, the magnetic axis at $\cong$ 3m, plasma minor radius $\cong$ 0.9 m and elongation $\cong$ 1.5. Figure 1 shows a representative pulse. The energy distribution of ICRH driven He^3 ions and NES driven deuterium ions were inferred from measurements made using the high energy NPA, the ion energy distribution functions inferred as described in [7,3].

The **L**ine-of-sight **I**ntegrated energy **D**istribution function (LID) inferred from the NPA measurements is that of trapped ions with pitch-angle $\vartheta \approx \pi/2 \pm 5\times10^{-3}$ and with ion speeds $v_Z >> (v_R, v_\phi)$, $v_Z (v_R, v_\phi) \geq 200$, as described in ref. [7,3]. Measurements from Pulse No: 553807 (measured LID of He^3 ions) and Pulse No: 53810 (measured LID of deuterium ions) are presented, as representative of all measurements for this study.

3. SELFO SIMULATION OF He^3 MINORITY ICRH AND OF HE3 ION ENERGY DISTRIBUTION FUNCTION

The SELFO code calculation of ICRH power absorption in the (R,Z) plane shows that the vertical NPA line-of-sight at R_{NPA} = 3.07m coincides with the ICRH absorption maximum. With the given magnetic field and ICRH frequency of 34MHz, the fundamental He^3 ICRH resonance was located at $R_{ICRH} \approx$ 3.08 m while the fundamental hydrogen minority resonance was outside the plasma on

the low-field side and the second harmonic hydrogen resonance (fundamental deuterium resonance) was close to the inner wall of the torus at $R \approx 2.3$m.

The computation of detailed He^3 ion velocity distribution function was performed using the SELFO Monte-Carlo code [8] which solves for the global wave field of the fast magnetosonic wave in a deuterium plasma containing minority He^3 ions with a self-consistent energy distribution function, such that the wave damping is balanced by the ICRH acceleration of the He^3 ions. The SELFO code models the distribution functions of the He3 ions using an orbit averaged Fokker Planck equation including Coulomb collisions and quasi-linear interactions with the fast magnetosonic wave. The SELFO He^3 distribution function) $f(R, Z, v_\perp, v_u)$ was input into the FPP-3D code. Figure 2 shows the resulting He3 ion distribution plotted as function of ion energy and ion pitch-angle, and fig.3 shows the resulting LID of the He3 minority ions.

4. FPP-3D SIMULATION OF NES DRIVEN DEUTERIUM ION ENERGY DISTRIBUTION FUNCTION

After being 'knocked-on' from the population of thermal ions the suprathermal D ions slow down due to Coulomb collisions with thermal electrons and ions. Their distribution function for energies high above the thermal can be determined using a kinetic equation. The 3D trajectory-averaged kinetic equation for the deuterium ion velocity distribution function, using a 3D collision operator that includes NES on He^3, was given in [2, 5, 9]; the equation includes drag and diffusion in velocity space, neoclassical ion transport, pitch-angle scattering and Coulomb collisions with the majority plasma electrons and ions, both Maxwellian. The kinetic equation is incorporated into the FPP-3D code to compute the evolution of initially Maxwellian deuterium ion distribution under the influence of NES with MeV energy ICRH driven He^3 ions.The trajectory averaged source term in the kinetic equation accounts for NES of He^3 projectile ions on deuterium target ions, as described in ref. [5]. The source represents the phase-space density of suprathermal deuterium ions produced in unit time due to NES. The reaction rates for NES, required for computing the source term S_d in [5], are obtained from differential cross-section data given in ref. [10]. Fig.4 shows the reaction rates obtained.

5. COMPARISON OF MEASURED AND SIMULATED LID OF DEUTERIUM ION ENERGY DISTRIBUTION

FPP-3D calculates the LID of deuterium ions corresponding to the NPA measurements from the 3D distribution function of all deuterium ions. The LID for other ions which occur in the FPP-3D simulations, i.e. He^3 ions, DT fusion α-particles, and other plasma ions can similarly be calculated. Fig.8 shows the calculated LID.

6. CONTRAST WITH SIMULATIONS OF DEUTERIUM TAIL DUE TO NES ON DT FUSION α-PARTICLES

The main results of measurement of suprathermal deuterium ion energy distribution, due to NES

on DT fusion -particles in JET plasmas, were presented in ref. [3]. A simplified analytical 1-D energy distribution for the suprathermal tail was calculated, using measured plasma parameters and an analytical solution of a 1-D slowing-down DT fusion -particle distribution. Comparison between the 1-D calculation of the LID and that inferred from NPA measurements showed reasonable agreement [3]. The result of the simplified calculation wasreinforced with simulation using the FPP-3D code in ref. [5]; the result is shown in fig.9.

CONCLUSIONS

- Contrasting the two experiments we deduce that the observed excess suprathermal D-ion population arises from NES processes with agents in addition to the He^3 ions which are not incorporated in the FPP-3D simulations.
- Plausible candidates are products of the (He^3+D) fusion reaction. Looking at the ICRH driven He^3 ion energy distribution in fig.2, and the energy dependence of the (He^3+D) fusion reaction rate in fig.4, we estimate that in the plasmas under consideration the (He^3+D) fusion rate will greatly exceed the (He^3+D) NES rate. We conjecture that the products of (He^3+D) fusion, 14.7 MeV protons and 3.6 MeV He4 ions, are the additional drivers of NES giving the observed excess suprathermal deuterium ions.
- Investigations of the NES tail formation in the presence of several sources of energetic projectile ions coupled through the fusion reaction will be the subject of future work. The investigation reported here and discussion of the results points to the need, when modeling the total fusion reactivity of ITER plasmas with He^3 ICRH, of taking account of NES of (D+He^3) fusion born alpha-particles and protons as additional drivers of suprathermal fuel ions, and booster of DT fusion reactivity.

ACKNOWLEDGEMENTS

Work at the UKAEA was funded jointly by the UK Engineering and Physical Sciences Research Council and by EURATOM. Work at Moscow State University was funded partly by the Russian Foundation for Basic Research under grants 07-07-00064, SS-1349.2003.1. The views and opinions expressed herein do not necessarily reflect those of the European Commission.

REFERENCES

[1]. Ryutov, D., *Physica Scripta* **45**(1992)153
[2]. Helander, P., Lisak, M. and Ryutov, D., *Plas. Phys. Contr. Fus.* **35** (1993) 363.
[3]. Korotkov, A., Gondhalekar, A. et al., *Physics of Plasmas* **7** (2000) 957.
[4]. Källne, J., Ballabo, L., Frenje, J., et al. *Physical Review Lett.* **85** (2000) 1246.
[5]. Zaitsev, F.S., Akers, R.J. and O'Brien, M.R.,'*Nuclear Fusion* **42** (2002) 1340.
[6]. Zaitsev, F.S., et al. 2007, *Plasma. Physics and Controlled Fusion* **49** (2007) 1747.
[7]. Korotkov, A., Gondhalekar, A., et al., *Nuclear Fusion* **37** (1997)35.
[8]. Hedin, J., Hellsten, T., Eriksson, L-G., and Johnson, T., *Nuclear Fusion* **42** (2002) 527.

[9]. Zaitsev, F.S., “Mathematical Modeling of Toroidal Plasma Evolution”, MAX Press, Moscow (2005) (in Russian).

[10]. Perkins, S.T. and Cullen, D.E.”*Nuclear Science and Engineering* **77** (1981) 20.

[11] Kiptily, V. G., Cecil, F. E., Jarvis, O. N., et al., *Nuclear Fusion* **42** (2002) 999.

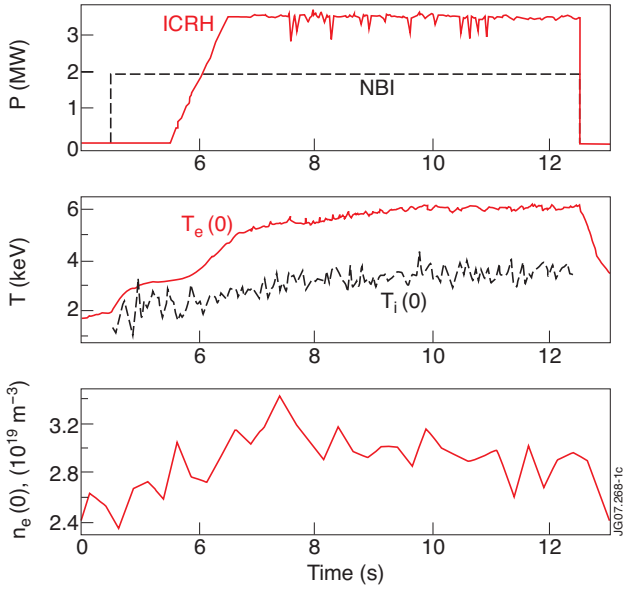

Figure 1: Shows time evolution of key plasma and heating parameters for JET Pulse No: 53807. Top box - Waveform of applied ICRH and NBI heating power; middle box - on-axis electron temperature T_e (0) measured using electron cyclotron emission, and ion temperature T_i (0) measured using charge-exchange spectroscopy; bottom box - on-axis electron density n_e (0) measured using Thomson scattering. At $t \geq 9.5$s into the pulse T_e (0), T_i (0) and n_e (0) are in steady-state. Time point $t = 9.5$s is chosen for the NPA measurement and the simulations discussed in the following.

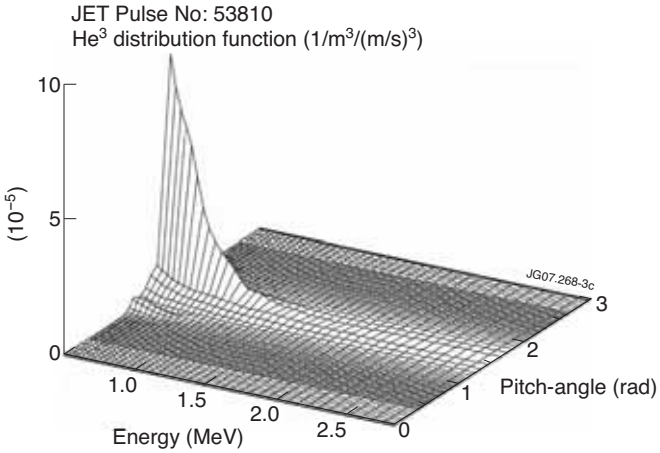

Figure 2: shows the SELFO + FPP-3D code calculation of the He^3 ion energy distribution function at t=9.5s, on flux-surface with γ= 0.5m, at poloidal angle $\vartheta \approx \pi/2$ (top of the flux-surface), as function of ion energy and pitch angle. Clearly, the majority of He^3 ion population is at energy E < 1MeV, and peaked at pitch-angles $\vartheta \approx \pi/2$.

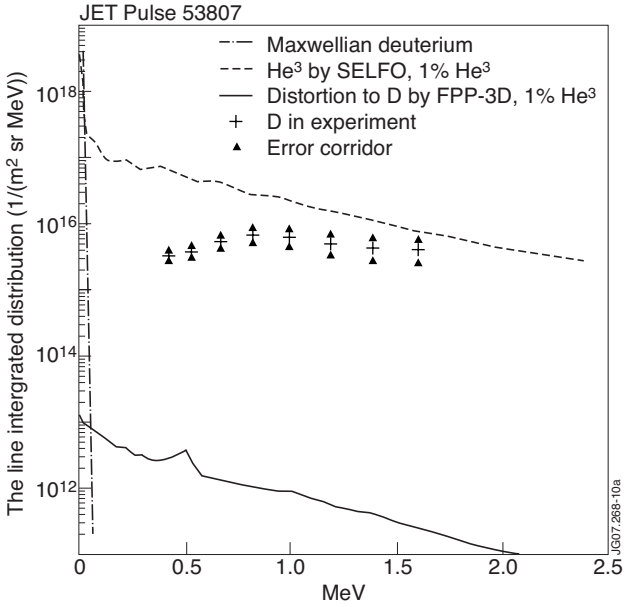

Figure 3: Shows the LID of He^3 ions inferred from NPA measurements, using measured bare impurity ion densities and other plasma parameters. The NPA measures ions with their turning point on the vertical line-of-sight [3, 7]; the NPA line-of-sight and the region of ICRH absorption overlapped. The SELFO code simulation of the LID of He^3 ions is also shown

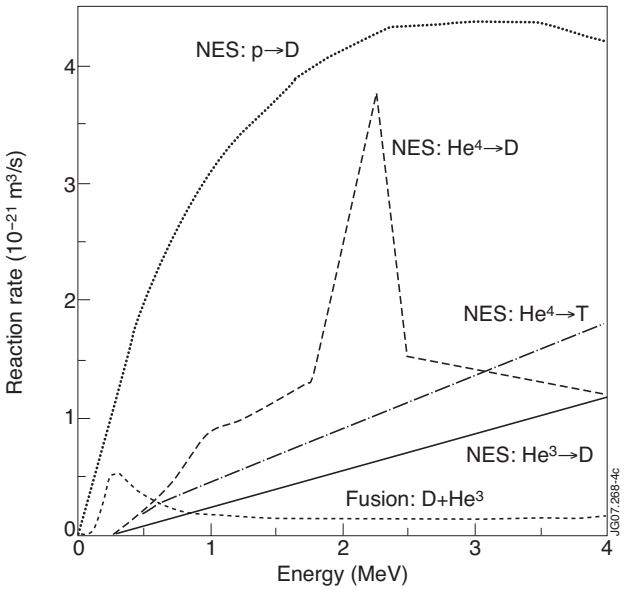

Figure 4: Shows the reaction rates in the energy range of interest. Comparing fig.2 and fig.4 we see that the ICRH driven He^3 ions overlap in energy the region of maximum in reaction rate for the fusion reaction $D + He^3 \rightarrow p(14.7\ MeV) + He^4\ (3.6MeV)$, ensuring efficient copious creation of new MeV energy ions.

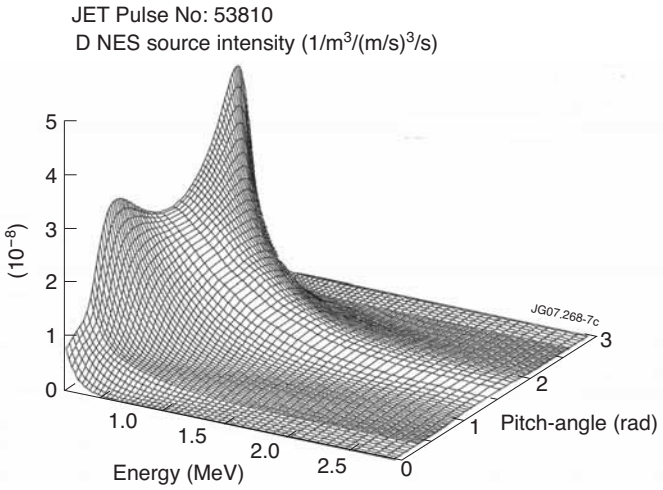

Figure 5: Shows the FPP-3D calculated NES deuterium source d S at minor radius $\gamma = 0.5$ and at poloidal angle $\pi/2$ (at top of the flux surface) as function of deuterium ion energy and pitch-angle. Comparing fig.5 with fig. 2 shows that a He^3 ion distribution that is narrow in pitch-angles gives rise to a NES deuterium ion source that is spread out in pitchangles. The calculations show also that (a) the source is spread out spatially, most contribution coming from region $0.3 \leq \gamma/\gamma_a \leq 0.7$, and (b) in energy most contribution to the source comes from deuterium ions of energy $0.3 \leq E_d\,(MeV) \leq 1.3$.

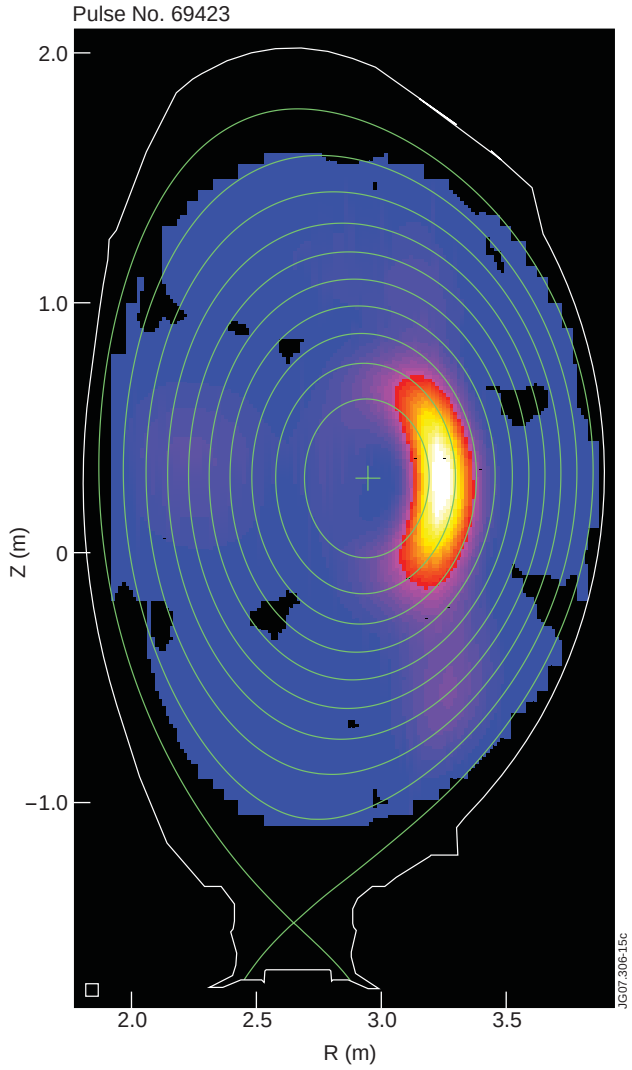

Figure 6: Shows a γ-ray image of the poloidal cross-section of JET plasma during He^3 minority ICRH. Regions of strong γ- ray emission are displayed. The γ-rays, in the range 2-7MeV, arise due to collisions between plasma impurity ions of C and Be and high energy ICRH driven He^3 ions, as described in ref. [11]. The observed γ-ray emission arises from the reactions $^{12}C(^3He, p\gamma)^{14}N$, $^9Be(^3He, n\gamma)^{11}C$ and $^9Be(^3He,p\gamma)^{11}B$. The nuclear reactions require that the He3 ion satisfy $E(He^3) > 0.8$ MeV. The figure thus illustrates the spatial location of regions of highest He^3 ion density, and the spatial profile of the NES deuterium source, reinforcing FPP-3D results.

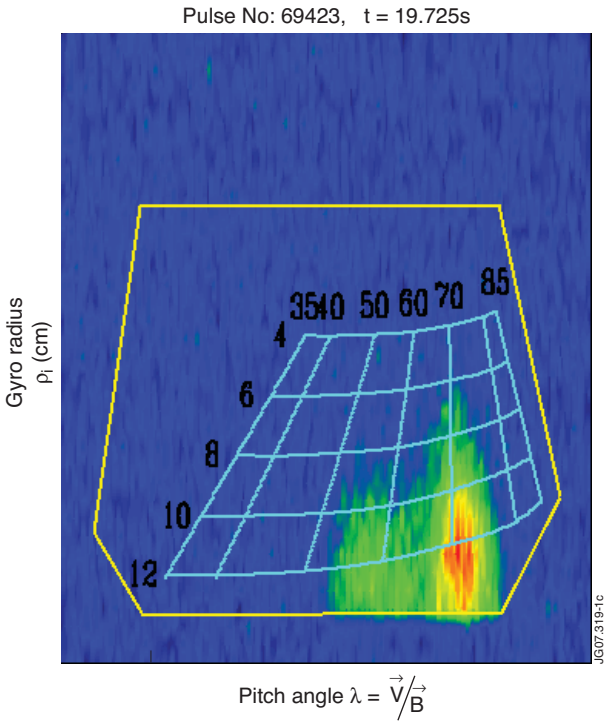

Figure 7: Measurements using a scintillator probe mounted outside the plasma at Z = −0.28m and R=3.84m. The dispersion in gyro-radius ρ_i and pitch-angle λ_i of escaped ions is shown. We infer that the detected ions are -particles from D + ^{3}He fusion reactions; their inferred energy, $3.1 \leq E(MeV) \leq 6.2$, is consistent with fusion of 3He projectile ions with an energy distribution function with an effective temperature of ≈ 350 keV.

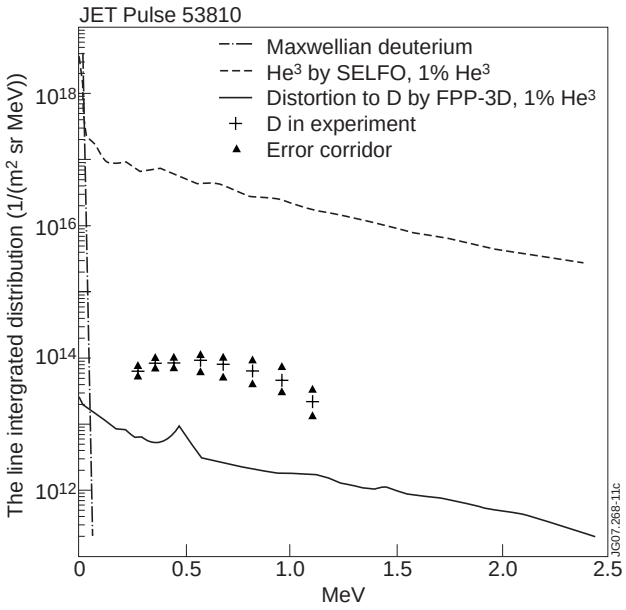

Figure 8: Shows the LID for the suprathermal tail of D-ions inferred from NPA measurements in Pulse No: 53810, compared with LID for deuterium ions, including the NES on ICRH driven He^3 ions, simulated using the FPP-3D code. Comparing the two LIDs we conclude that the FPP-3D simulation underestimates the density of the suprathermal deuterium ions. The excess suprathermal deuterium ion population lies outside the uncertainties in the FPP-3D simulations and those in the LID inferred from NPA measurements.

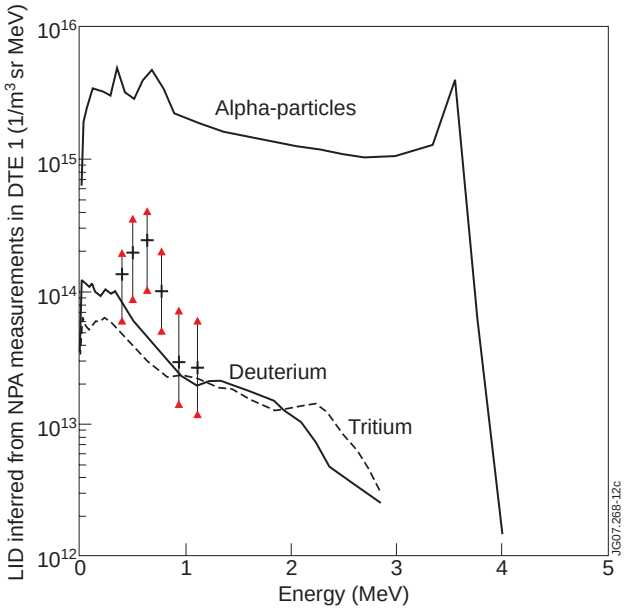

Figure 9: Shows a contrasting comparison between the measured LID of suprathermal deuterium ion energy distribution function arising due to NES with DT fusion α-particles, and simulation of it using the FPP-3D code. Credible agreement between the two may be claimed.